Electronic Supplementary Material (ESI) for Polymer Chemistry.

Supporting Information

Phase Separation and Self-Assembly of Cyclic Amphiphilic Block Copolymers with a Main-Chain Liquid Crystalline Segment

Satoshi Honda, Maito Koga, Masatoshi Tokita,* Takuya Yamamoto,*

and Yasuyuki Tezuka*

Department of Organic and Polymeric Materials, Tokyo Institute of Technology,

O-okayama, Meguro-ku, Tokyo 152–8552, Japan

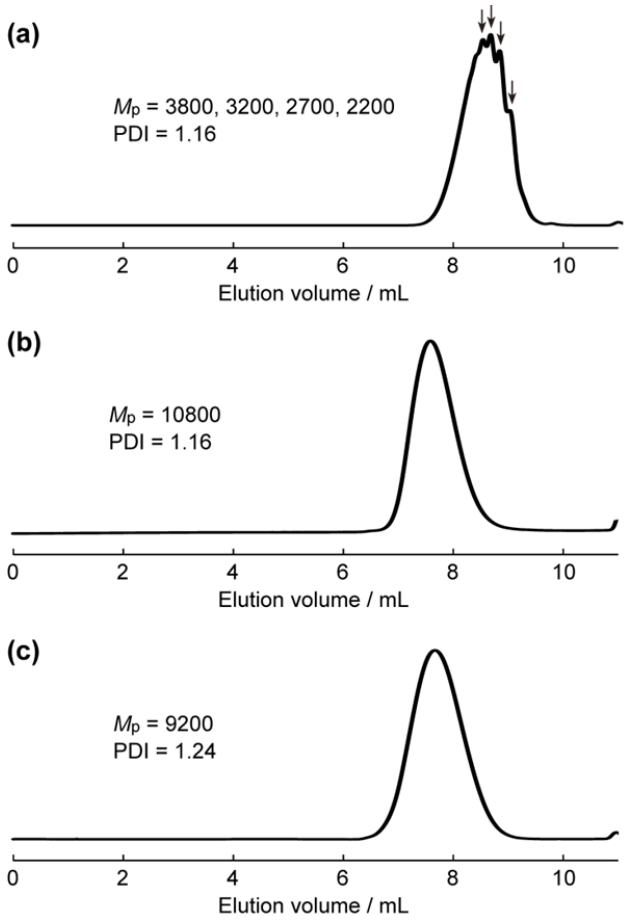

Figure S1. SEC traces of (a) a SEC-fractionalized BB_9 macroinitiator, (b) linear $t\mathrm{BA}_{21}\mathrm{BB}_9t\mathrm{BA}_{21}$, and (c) cyclic $t\mathrm{BA}_{31}\mathrm{BB}_{10}$.

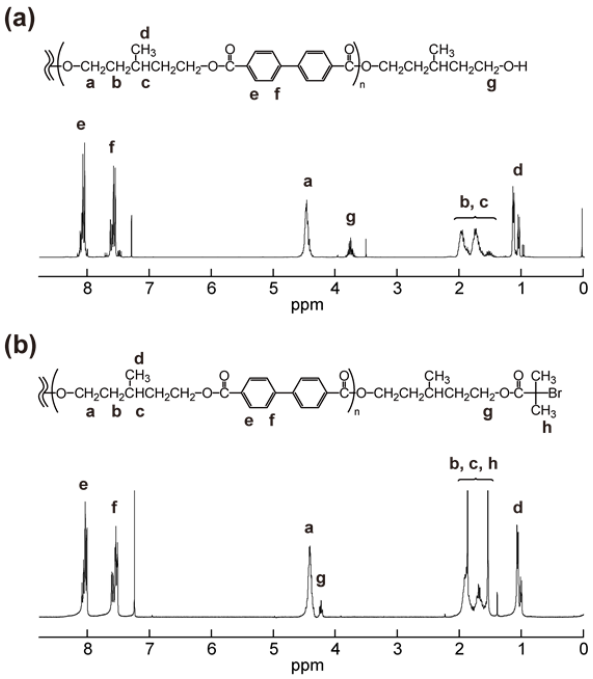

Figure S2. ^{1}H NMR spectra of (a) hydroxyl-terminated BB_n and (b) a SEC-fractionated BB_9 macroinitiator.

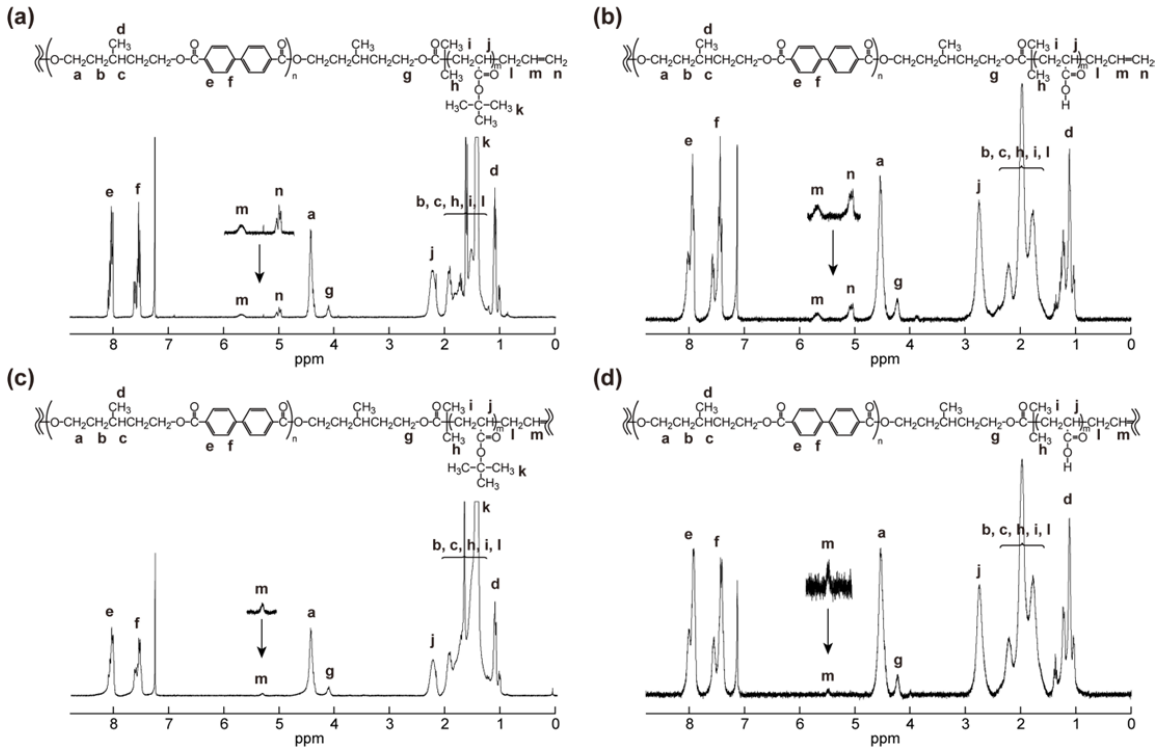

Figure S3. ^{1}H NMR spectra of (a) linear $t\mathrm{BA}_{21}\mathrm{BB}_{9}t\mathrm{BA}_{21}$, (b) cyclic $t\mathrm{BA}_{31}\mathrm{BB}_{10}$, (c) linear $\mathrm{AA}_{21}\mathrm{BB}_{9}\mathrm{AA}_{21}$, and (d) cyclic $\mathrm{AA}_{33}\mathrm{BB}_{10}$.

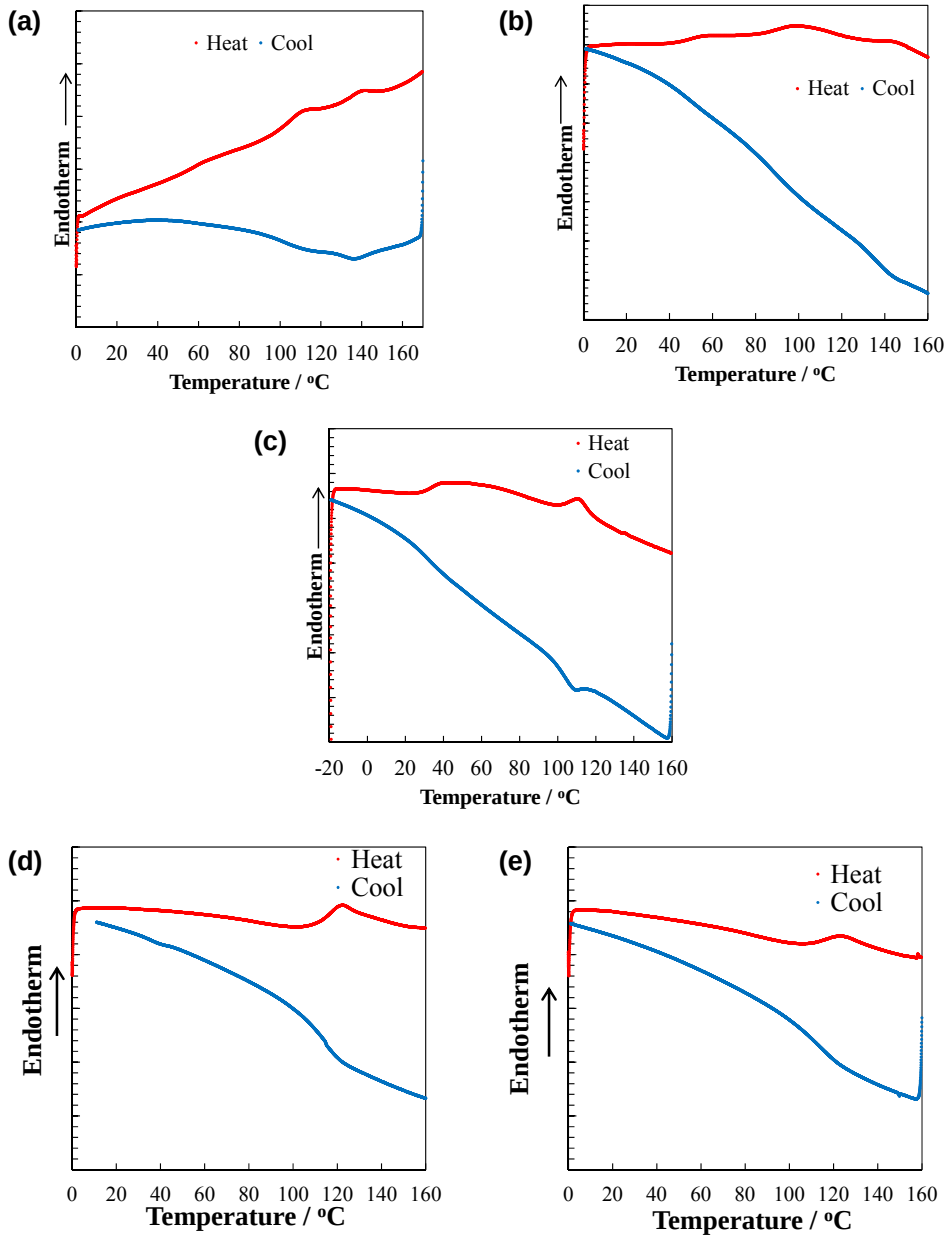

Figure S4. DSC thermograms of (a) linear $AA_{21}BB_9AA_{21}$, (b) cyclic $AA_{33}BB_{10}$, (c) cyclic $AA_{51}BB_{18}$, (d) linear $AA_{44}BB_9AA_{44}$, and (e) cyclic $AA_{100}BB_9$.

Table S1. T_i, $T_{g,\ AA}$, $T_{g,\ BB}$, and ΔH_i of linear $AA_{21}BB_9AA_{21}$, cyclic $AA_{33}BB_{10}$, cyclic $AA_{51}BB_{18}$, linear $tBA_{50}BB_8tBA_{50}$, linear $AA_{44}BB_9AA_{44}$, and cyclic $AA_{100}BB_9$

	$T_{g,\ BB}$ (°C)	$T_{g,\ AA}$ (°C)	T_i (°C)	ΔH_i (kJ mol^{-1})
linear $AA_{21}BB_9AA_{21}$	58	106	140	0.56
cyclic $AA_{33}BB_{10}$	49	94	145	0.50
cyclic $AA_{51}BB_{18}$	33	-	111	2.33
linear $tBA_{50}BB_8tBA_{50}$	37	-	-	-
linear $AA_{44}BB_9AA_{44}$	-	114	-	-
cyclic $AA_{100}BB_9$	-	115	-	-

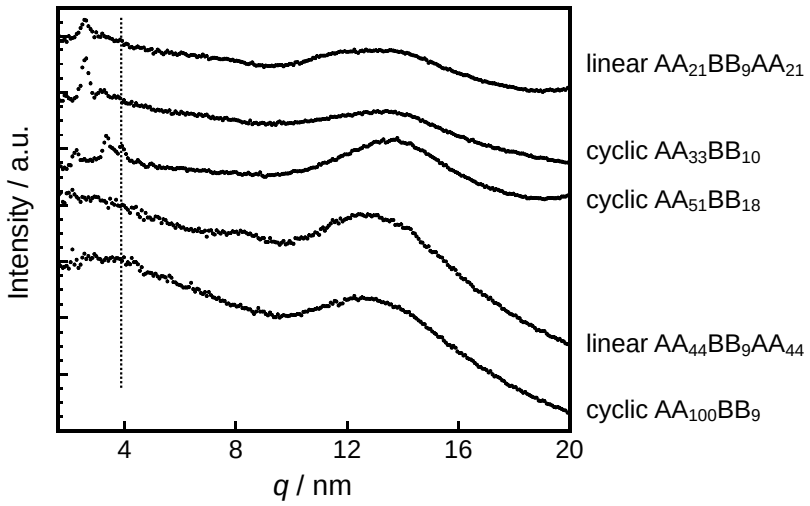

Figure S5. WAXD intensity profiles of linear $AA_{21}BB_9AA_{21}$, cyclic $AA_{33}BB_{10}$, cyclic $AA_{51}BB_{18}$, linear $AA_{44}BB_9AA_{44}$, and cyclic $AA_{100}BB_9$. The dashed line marks the peak position of smectic layer reflection (q = 3.86 nm^{-1}). The reflections at q < 3.86 nm^{-1} are ascribed to the lamellar microdomains.

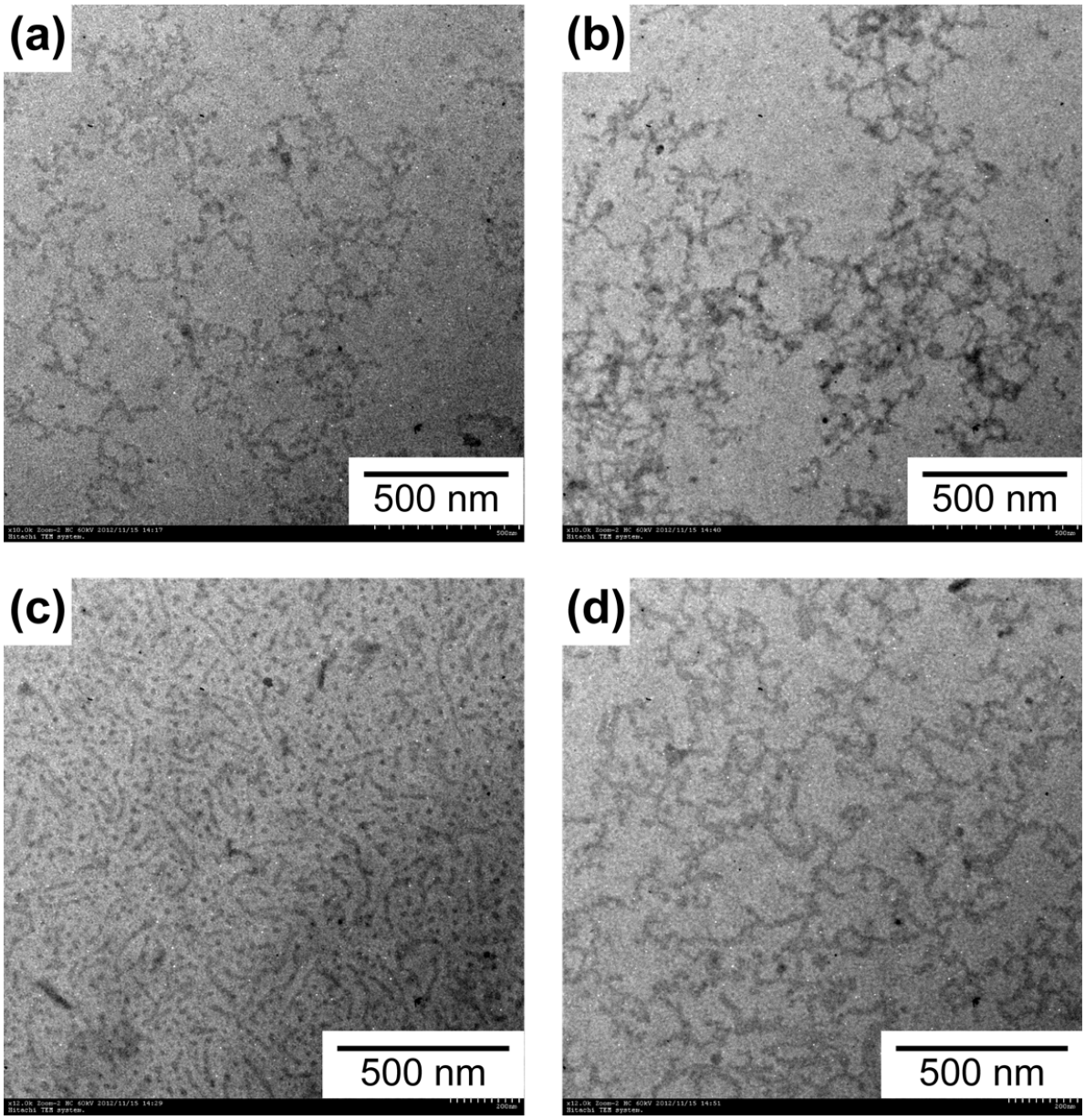

Figure S6. TEM images of self-assembled structures from linear $AA_{21}BB_9AA_{21}$ and cyclic $AA_{33}BB_{10}$ using an initial THF solution with a polymer concentration (c_0) of 1.0 and 10 mg/mL. (a) Linear, c_0 = 1.0 mg/mL. (b) Cyclic, c_0 = 1.0 mg/mL. (c) Linear, c_0 = 10 mg/mL. (d) Cyclic, c_0 = 10 mg/mL.

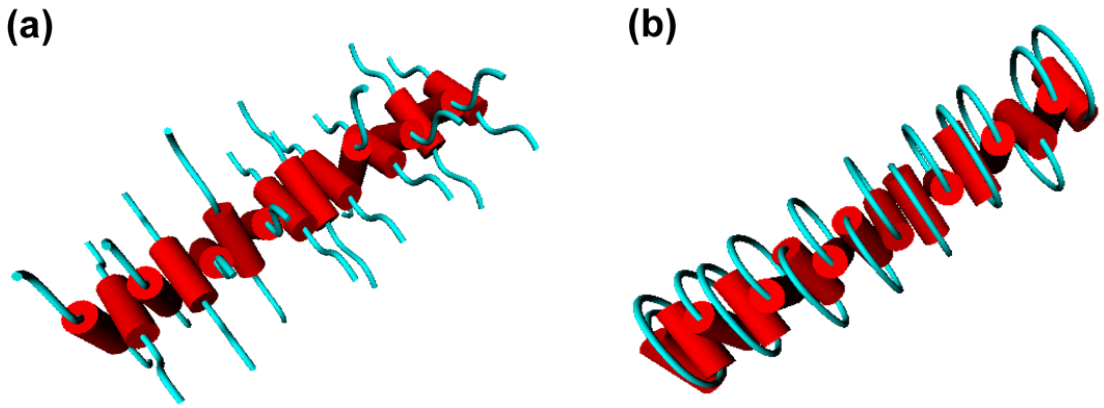

Figure S7. Models for cylindrical micelles self-assembled from (a) linear $AA_{21}BB_9AA_{21}$ and $AA_{25}BB_{14}AA_{25}$ and (b) cyclic $AA_{33}BB_{10}$ and $AA_{51}BB_{18}$. Light blue and red indicate $AA_{(2)m}$ and BB_n segments, respectively.

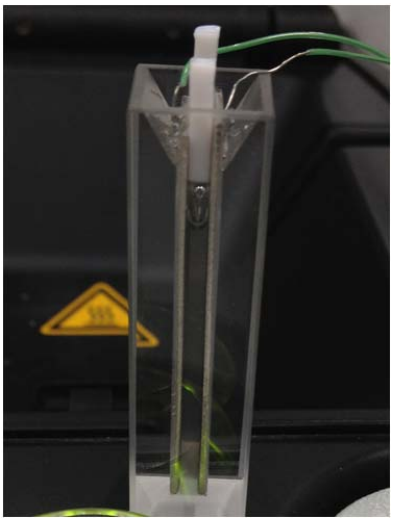

Figure S8. A photograph for an experimental setup to apply an electric field. Two platinum plates (10 mm × 40 mm × 1.0 mm) were equipped to the inside walls of a quartz cell facing each other with 2 mm separation. Wire leads were soldered to the platinum plates to connect to a Kawaguchi Electric Works V7032A high voltage DC power supply. A suspension (0.4 mL) of self-assembled linear $AA_mBB_nAA_m$, cyclic $AA_{2m}BB_n$, or linear $AA_{134}St_{34}AA_{134}$ was added to the cell, and electric field was applied at 1.5 V/mm for 2 min.

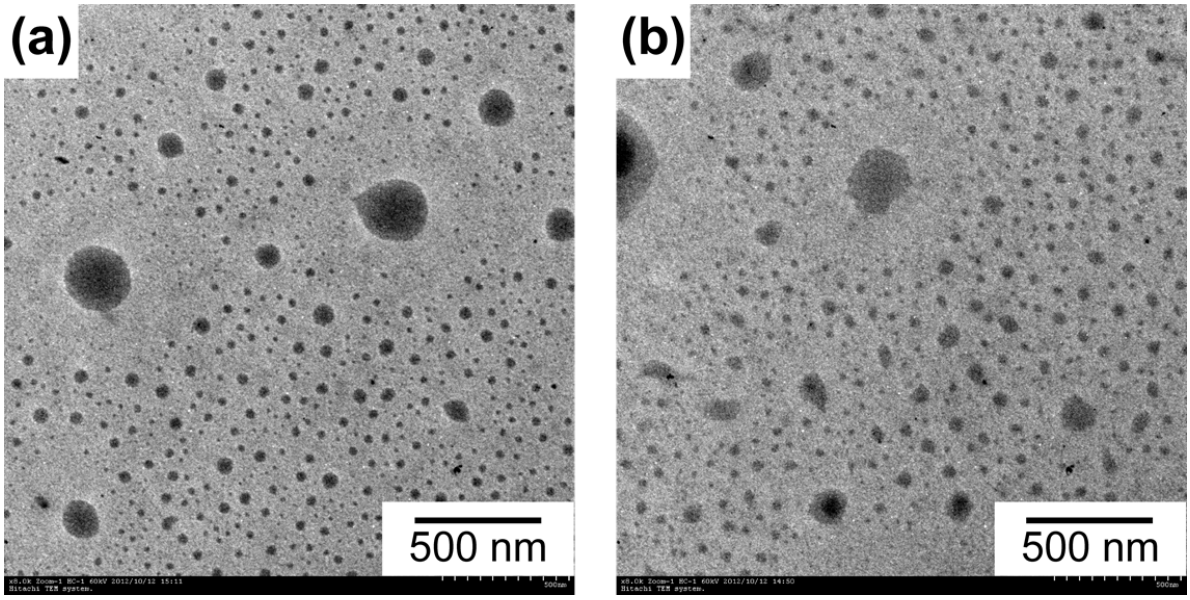

Figure S9. TEM images of self-assembled structures from linear $AA_{134}St_{34}AA_{134}$ (a) before and (b) after applying an electric field of 1.5 V/mm for 2 min.